Bioorganic & Medicinal Chemistry 21 (2013) 379–387

Contents lists available at SciVerse ScienceDirect

Bioorganic & Medicinal Chemistry

journal homepage: www.elsevier.com/locate/bmc

Synthesis and in vitro biological evaluation of lipophilic cation conjugated photosensitizers for targeting mitochondria

Pallavi Rajaputra, Gregory Nkepang, Ryan Watley, Youngjae You *

College of Pharmacy, University of Oklahoma Health Sciences Center, Oklahoma City, OK 73117, United States
Department of Chemistry and Biochemistry, University of Oklahoma, Norman, OK 73019, United States

ARTICLE INFO

Article history:
Received 16 October 2012
Revised 21 November 2012
Accepted 23 November 2012
Available online 3 December 2012

Keywords:
Mitochondria targeting conjugates
Delocalized cationic dye
Photodynamic therapy
Anticancer therapy

ABSTRACT

Mitochondria-specific photosensitizers were designed by taking advantage of the preferential localization of delocalized lipophilic cations (DLCs) in mitochondria. Three DLC-porphyrin conjugates: CMP-Rh (a core modified porphyrin-rhodamine B cation), CMP-tPP (a core modified porphyrin-mono-triphenyl phosphonium cation), CMP-$(tPP)_2$ (a core modified porphyrin-di-tPP cation) were prepared. The conjugates were synthesized by conjugating a monohydroxy core modified porphyrin (CMP-OH) to rhodamine B (Rh B), or either one or two tPPs, respectively, via a saturated hydrocarbon linker. Their ability for delivering photosensitizers to mitochondria was evaluated using dual staining fluorescence microscopy. In addition, to evaluate the efficiency of the conjugates as photosensitizers, their photophysical properties and in vitro biological activities were studied in comparison to those of CMP-OH. Fluorescence imaging study suggested that CMP-Rh specifically localized in mitochondria. On the other hand, CMP-tPP and CMP-$(tPP)_2$ showed less significant mitochondrial localization. All conjugates were capable of generating singlet oxygen at rates comparable to CMP-OH. Interestingly, all cationic conjugates showed dramatic increase in cellular uptake and phototoxicity compared to CMP-OH. This improved photodynamic activity might be primarily due to an enhanced cellular uptake. Our study suggests that Rh B cationic group is better at least for CMP than tPP as a mitochondrial targeting vector.

1. Introduction

Photodynamic therapy (PDT) has gained great popularity as a treatment modality for both neoplastic and non-neoplastic diseases. A beauty of PDT lies in its ability to ablate malignant tissue without systemic toxicity, which is a major drawback of traditional methods like chemotherapy and radiotherapy. PDT involves an energy transformation from photonic energy (light) to chemical energy (reactive singlet oxygen) via a non-toxic photosensitizer. Singlet oxygen ($^1O_2$) is the principal cytotoxic agent in PDT.[1,2] Due to the short lifetime (<0.04 μs) and small radius of diffusion in biological systems (<0.02 μm),[3] the photosensitizer should be closely located to the target (the site of action) damaged by PDT.

Mitochondrion is a key organelle for cell survival due to its involvement in energy production and apoptotic pathways.[4–10] Hence, by targeting the mitochondria of the cell we may not only achieve apoptotic cell death but also maximize PDT effect. A number of photosensitizers have been designed to target the mitochondria of a cell for improved PDT treatment.[11] A few of them are benzoporphyrin-derivatives,[12] delocalized lipophilic cations (DLCs) like Rhodamine 123,[13] thiopyrylium AA-1,[14] Rhodacyanin MKT-077.[15] One popular strategy for targeting strategy is to take advantage of DLCs' tendency of preferential accumulation in mitochondria.[16–21] DLCs penetrate the hydrophobic layer of plasma and mitochondria membrane and accumulate inside the mitochondria. According to Nernst equation every 60 mV difference in membrane potential could lead to 10-fold increase in the accumulation of compounds bearing positive charge.[20] A maximum of ~180 mV of potential difference has been measured in the mitochondrial membrane.[22] Theoretically, up to 1000-folds more mitochondrial accumulation compared to extracellular fluid could be achieved based on the charge on the molecule.

In our previous report, we designed TPP-DLC (TPP: tetraphenyl porphyrin and DLC: rhodamine B or acridine orange) conjugates and achieved mitochondrial localization and higher cellular uptake by conjugating porphyrin to rhodamine B.[23] We obtained 8 and 14 times higher uptake with the conjugate compared to unconjugated porphyrin and rhodamine B, respectively. Core-modified porphyrins (CMPs) have been extensively studied as a second-generation photosensitizer due to their multiple advantages.[24–29] Especially, the dithiaporphyrins were prepared as a highly pure and well-characterized form. CMPs can also absorb longer wavelength light (690–710 nm) than Photofrin (a clinically approved photosensitizer, 630 nm) and tetra-pyrrole prophyrins (648 nm)[23] and are

* Corresponding author. Tel.: +1 405 271 6593; fax: +1 405 271 7505.
E-mail address: youngjae-you@ouhsc.edu (Y. You).

0968-0896/$ - see front matter © 2012 Elsevier Ltd. All rights reserved.
http://dx.doi.org/10.1016/j.bmc.2012.11.032

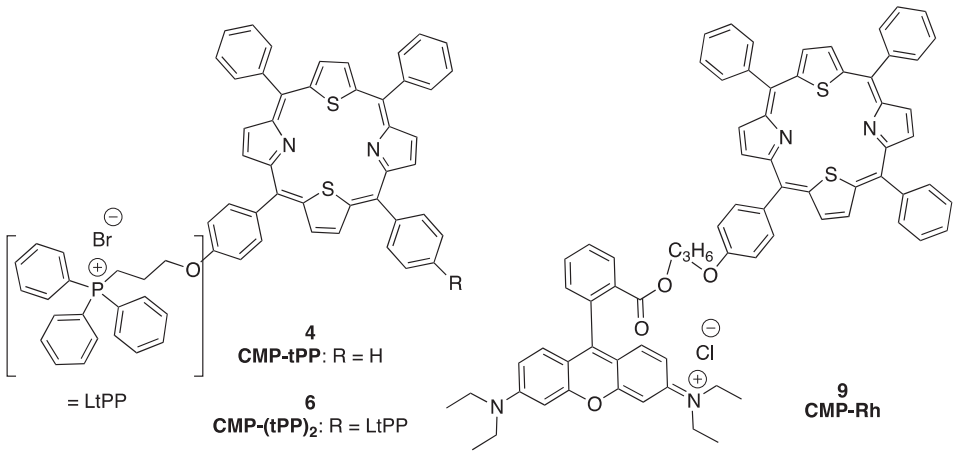

Figure 1. Structures of DLC-conjugated CMPs.

highly photostable.[30] In addition, CMPs showed high singlet oxygen generation quantum yield ($\Phi(^1O_2)$, ~0.8) making them very efficient PS for PDT treatment.[27]

In the current work, we attempted to develop mitochondria-specific CMP conjugates by tethering it to DLCs. Three conjugates were designed such as CMP-Rh (**9**, a core modified porphyrin-rhodamine B), CMP-tPP (**4**, a core modified porphyrin-mono-triphenyl phosphonium), and CMP-$(tPP)_2$ (**6**, a core modified porphyrin-di-triphenyl phosphonium cation) (Fig. 1). The choice of rhodamine B is mainly due to its effective delivery of photosensitizers (tetraphenyl porphyrin (TPP) and phthalocyanine (Pc)) into the mitochondria.[23,31] tPP was chosen since it also improved the mitochondrial uptake of several bioactive compounds by several hundred folds.[32–35] We prepared both mono- and di-substituted CMP-tPPs to see the effect of a number of cation on mitochondrial localization. We envisioned that these DLCs deliver the conjugates to mitochondria and thus eventually augment the PDT efficiency of CMP.

2. Results and discussion

2.1. Synthesis

Three conjugates, CMP-tPP and CMP-$(tPP)_2$, and CMP-Rh containing one or two delocalized lipophilic cation groups, were synthesized to target the mitochondria (Scheme 1). Although conjugates CMP-tPP and CMP-Rh were synthesized from CMP-OH, the procedures differed slightly following the alkylation to give **3**. For CMP-Rh, **3** was reacted with sodium acetate in anhydrous DMF under reflux to give **7**. This was then hydrolyzed to give alcoholic compound **8** that was conjugated to Rh B by esterification to afford the pure final product **9** in 38% yield. For CMP-tPP and CMP-$(tPP)_2$, phenolic CMPs **1** and **2** were alkylated to give **3** and **5**. CMP-tPP and CMP-$(tPP)_2$ were obtained by reactions of alkyl bromides **3** and **5** with triphenyl phosphine in 47% and 22% yield, respectively. These reactions took several days (88 and 96 h), probably due to steric hindrance in the dyes. The final compounds were unambiguously characterized by ^{1}H NMR and high Mass.

2.2. Photophysical studies

2.2.1. Absorption spectra and molar extinction coefficients

Three conjugates showed all the characteristic absorption peaks of its respective components, indicating that no significant electronic interactions might occur at the ground state (Fig. 2).[36] While absorption maxima and extinction coefficient of all the conjugates remained practically the same, the extinction coefficients of CMP-OH had much lower molar extinction coefficients than those of the others (Table 1). It might indicate some degree of aggregation in the ground state.[37] There was a slight red shift of Rh B peak from 550 to 558 nm in CMP-Rh as observed in our previous conjugate TPP-Rh. This might be due to the proximity of the CMP moiety that seemed to change the polarity of the environment of rhodamine moiety, consequently red shifting the maxima of Rh B in the conjugate.[38,39]

2.2.2. Aggregation tendency of the dyes

Generally, the aggregation tendency of a dye is greatly dependent on various factors such as lipophilicity, molecular symmetry, and flexibility.[37] Aggregation usually leads to a dramatic decrease in both fluorescence emission and singlet oxygen generation, consequently decreasing the photodynamic activity of photosensitizers.[40] High aggregation tendency in a medium could be translated to that in the cytoplasm. Consequently, it could cause reduced phototoxicity. Although the lipophilicities ($\mathrm{Log}D_{7.4}$) of the dyes are pretty close, within 1.79–2.04, their aggregation tendencies in the medium showed variations (Fig. 3). All three conjugates seemed to aggregate more in aqueous media and less in DMSO. CMP-OH showed the most severe aggregation in the medium, only 2.5% fluorescence emission in the medium compared to that in DMSO. This suggests that the aggregation of the conjugates could be attributed mostly to the highly planar and rigid structure of CMP-OH. However, Rh B and CMP-Rh showed a different aggregation pattern, aggregating almost similar in both medium and DMSO. This is probably due to the presence of the rotatable pendant phenyl ring of rhodamine B moiety thus reducing the aggregation in the medium.

2.2.3. Energy transfer in the conjugate CMP-Rh

Energy transfer (ET), a communication between two chromophores, is a possible phenomena when the two chromophores are in proximity. Among the three conjugates, only CMP-Rh has two chromophores with a potential of ET. We also observed ET between TPP and Rh.[23] If there is ET from CMP to Rh, it could reduce singlet oxygen generation capability of CMP of the CMP-Rh. Thus, to estimate ET we measured fluorescence quenching in three samples: (1) CMP-Rh (2) CMP-OH (or Rh B), and (3) a mixture of CMP-OH and Rh B at an equimolar concentration (2 μM). If there is ET, fluorescence of excited chromophores should be reduced. Fluorescence emission spectra were recorded after irradiation at 435 or 525 nm to excite CMP or Rh moiety (Fig. 4).

Interestingly, when CMP of CMP-Rh was excited at 435 nm, it showed very similar CMP emission (λ_{max}, 705 nm) intensity with those of CMP-OH and a mixture of CMP-OH and Rh B (Fig. 4a).

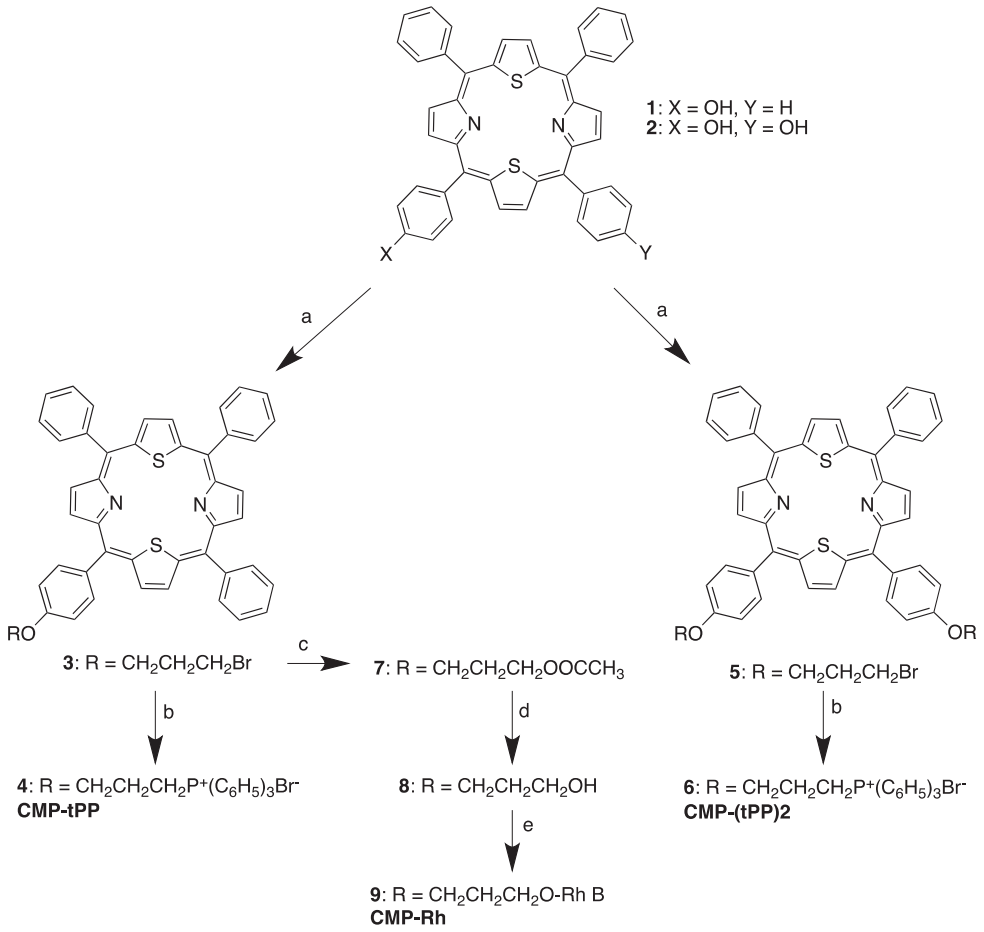

Scheme 1. Reagents and conditions: (a) excess $BrCH_2CH_2CH_2Br$, 20 equiv K_2CO_3, acetone, 80 °C, 36 h (b) 1.2 equiv triphenyl phosphine, absolute ethanol, 85 °C, 88–96 h (c) 5 equiv Na^+–$OOCCH_3$, anhydrous DMF, 90 °C, 12 h (d) 0.5 N NaOH, THF:MeOH:H_2O (v/v/v: 1.3:2.5:0.75), 80 °C, overnight (e) 1.1 equiv Rhodamine B, 0.11 equiv DMAP, and 1.1 equiv DCC, CH_2Cl_2, 0 °C to rt, 72 h.

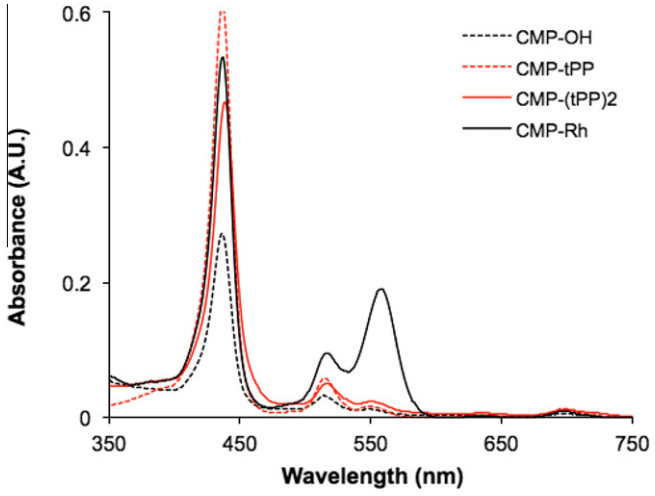

Figure 2. Absorption spectra of CMP-OH, CMP-tPP, CMP-$(tPP)_2$, and CMP-Rh at 2 μM in $CHCl_3$.

There might be no significant energy loss in CMP-Rh when excited at CMP. On the other hand, when Rh of CMP-Rh was excited at 525 nm, there was dramatic decrease (~80%) in fluorescence emission from CMP-Rh compared to those of Rh B and a mixture of CMP-OH and Rh B (Fig. 4b). In addition, after excitation at Rh group at 525 nm, a significant CMP emission was detected from CMP-Rh but not from CMP-OH + Rh B (Fig. 4c). There might be a ET from Rh to CMP. Since there may not be effective energy transfer from CMP to Rh, it is unlikely that singlet oxygen generation capability of CMP in CMP-Rh is reduced.

2.2.4. Singlet oxygen generation

Singlet oxygen generation efficiency of the photosensitizers was evaluated using DPBF (1,3-diphenylisobenzofurane), a popular singlet oxygen probe.[41] The rates of DPBF oxidation by all three conjugates were similar to that of CMP-OH (Fig. 5). Even CMP-Rh and CMP-$(tPP)_2$ showed faster DPBF oxidation. In our previous studies, CMPs gave high effective singlet oxygen quantum yields, ~0.8.[42–44] This indicates all conjugates were able to generate singlet oxygen at rates comparable to that of CMP-OH with CMP-Rh being the most efficient followed by CMP-$(tPP)_2$. No significant DPBF oxidation was detected by light alone, Rh B, or tPP alone.

2.3. Biological studies

2.3.1. Cellular uptake

Cellular uptake was determined using the fluorescence of the conjugates after colon 26 cells were incubated with each conjugate for 24 h at 5 or 10 μM. Interestingly, all three cationic conjugates showed greatly enhance uptake compared to the unconjugated dyes (CMP-OH or Rh B) (Fig. 6). CMP-Rh and CMP-$(tPP)_2$ showed about 7 times and CMP-tPP showed about 14 times higher than CMP-OH at 10 μM. Similarly, the conjugates CMP-Rh, CMP-tPP, CMP-$(tPP)_2$ showed 10.6, 18.9, 8.3 times higher uptake than

Table 1
UV–vis—near—IR band maxima and extinction coefficients in chloroform and *n*-octanol/pH 7.4 buffer partition coefficients of dyes

Compds	Soret band	Band IV	Band III	Band II	Band I	Log $D_{7.4}$
CMP-OH	436 (146)	517 (17.3)	548 (5.7)	636 (2.6)	699 (2.8)	2.3
CMP-tPP	437 (293)	515 (27.8)	549 (8.3)	634 (1.7)	698 (5.9)	2.04
CMP-$(tPP)_2$	438 (231)	516 (23.7)	551 (11.0)	634 (6.0)	700 (5.4)	1.79
CMP-Rh	437 (280)	517 (50.0)	558 (101.3)	NA	700 (4.4)	2.01
Rh B			550 (110.6)[a]			2.07

λ_{max}, nm ($\varepsilon \times 10^3\ M^{-1}\ cm^{-1}$).
[a] In methanol.

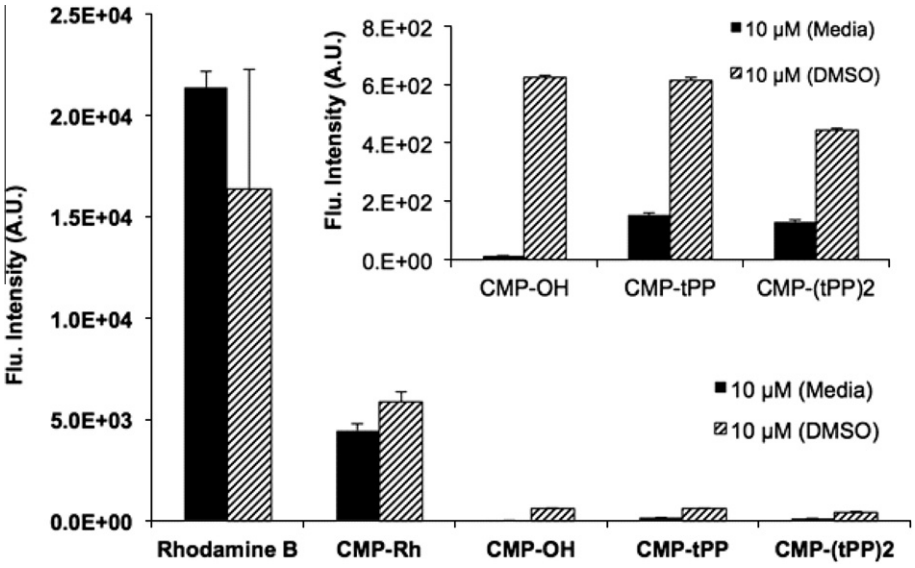

Figure 3. Fluorescence emission from the dyes (10 μM) in both the complete medium and DMSO: CMP-OH, CMP-tPP and CMP-$(tPP)_2$ excitation at 430 nm and emission at 714 nm and CMP-Rh and Rh B excitation at 520 nm and emission at 590 nm. Inset shows an expanded area.

CMP-OH at 5 μM. The higher accumulation of the conjugates compared to CMP-OH could be attributed to the delocalized positive charge on the molecules and reduced aggregation due to their increased flexibility by the aliphatic linker. The delocalized positive charge on the molecules might facilitate binding to negatively charged proteoglycan on cell membrane and allow diffusion into the cells and the mitochondria against the potential gradient.[45–48] The increased flexibility of the conjugate might contribute to the enhanced uptake at least in part by decreasing the aggregation and increasing the entropy of the conjugates.[49]

2.3.2. Dark toxicity

No significant dark toxicity was observed in cells treated with up to 5 μM of CMP-OH, Rh B, tPP or three conjugates (Fig. 7). This may probably be due to their inability to generate singlet oxygen in the dark.

2.3.3. Phototoxicity

The conjugates showed greatly increased phototoxicity compared to the unconjugated photosensitizer (CMP-OH) (Fig. 8). No significant phototoxicity was observed in cells treated with up to 5 μM of CMP-OH after irradiated with a 690 nm diode laser at 5.6 $mWcm^{-2}$ for 30 min. On the other hand, cells treated with 5 μM of either CMP-Rh, CMP-tPP or CMP-$(tPP)_2$ and irradiated under the same condition showed >70% cell killing. CMP-tPP showed the highest phototoxicity under the above irradiation conditions with an IC_{50} of 0.9 μM, followed by CMP-$(tPP)_2$ with an IC_{50} of 1.67 μM and then CMP-Rh with an IC_{50} of 2.36 μM. The absence of phototoxicity observed in the cells treated with up to 5 μM of CMP-OH could be attributed mainly to their low intracellular accumulation (0.19 fmole/cell). Rh B did not show any toxicity upto 5 μM as expected due to its inability to generate singlet oxygen. On the other hand, the greater phototoxicity observed with CMP-tPP, CMP-$(tPP)_2$, and CMP-Rh could be attributed to their high intracellular accumulation with effective singlet oxygen generation capability.

2.3.4. Sub-cellular localization

Since the conjugates were designed to target mitochondria, mitochondrial localization was estimated using fluorescence dual staining with mitochondrial molecular probe, Rhodamine 123 (Fig. 9). Green filter (excitation 480/40 emission 527/30) was used to obtain signal from Rhodamine 123. Red filter (excitation 535/50 emission 645/75) was used to obtain signal from CMP of the CMP conjugates.

CMP-Rh showed a very similar staining pattern to Rh-123 (Fig. 9c). CMP-Rh was distributed throughout the cytoplasm like Rh-123 (Fig. 9b). In addition, CMP-Rh and Rh-123 showed punctuate staining patterns consistent with typical mitochondrial probe images. This sub-cellular localization of CMP-Rh was further confirmed by the overlapping of the two images (Fig. 9d), where yellow area present co-localization of CMP-Rh and Rh 123. The CMP-Rh might be accumulated in mitochondria due to the presence of the delocalized lipophilic cation that facilitated their accumulation in mitochondria. On the other hand, CMP-tPP did not show any significant staining of mitochondria. Bright CMP fluorescence was detected from edges of cells. Very minimal yellowish area was shown (Fig. 9h). CMP-$(tPP)_2$ also showed some degree

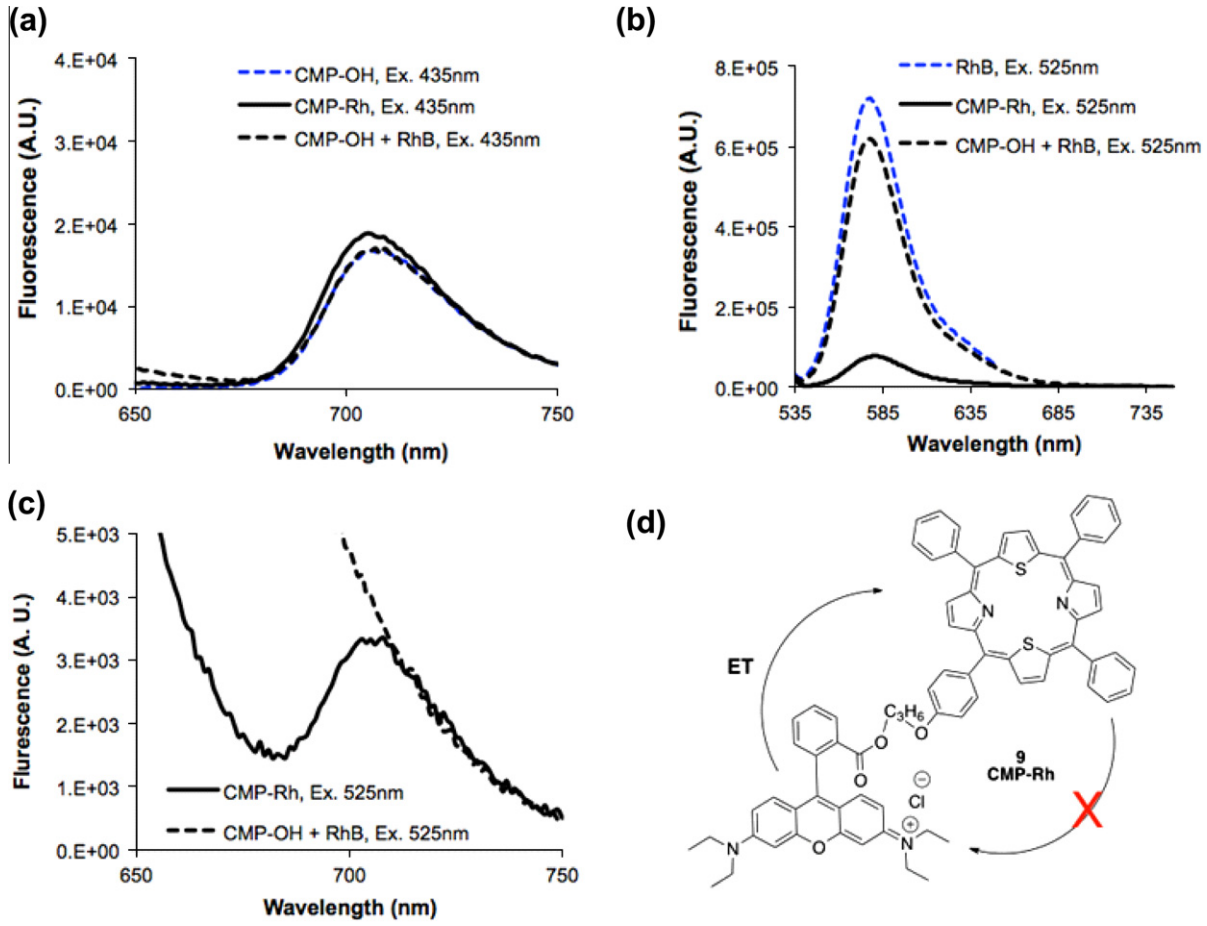

Figure 4. Fluorescence spectra of CMP-Rh, CMP-OH, and Rh B (a) excited at 435 nm, (b) excited at 525 nm, (c) magnified graph of b in the CMP emission peak area, and (d) ET directions in CMP-Rh.

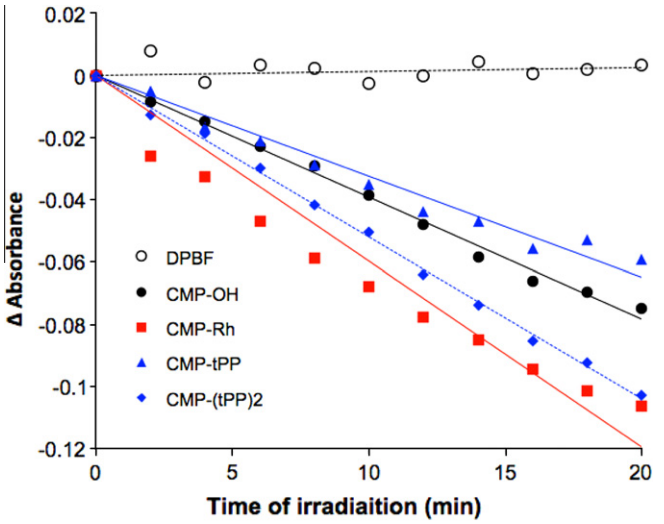

Figure 5. Relative rates of DPBF oxidation by singlet oxygen generated from the respective dyes irradiated with 690 ± 10 nm light (LC122-A, LumaCare) at 1 mWcm^{-2}. Five micrometer of the respective dyes were mixed with 100 μM of DPBF and the mixture irradiated for 20 min. Absorbance readings at 414 nm were taken every 2 min.

of mitochondrial localization. More yellowish areas (Fig. 9l) were shown than CMP-tPP (Fig. 9h). However, it was less than that of CMP-Rh (Fig. 9d).

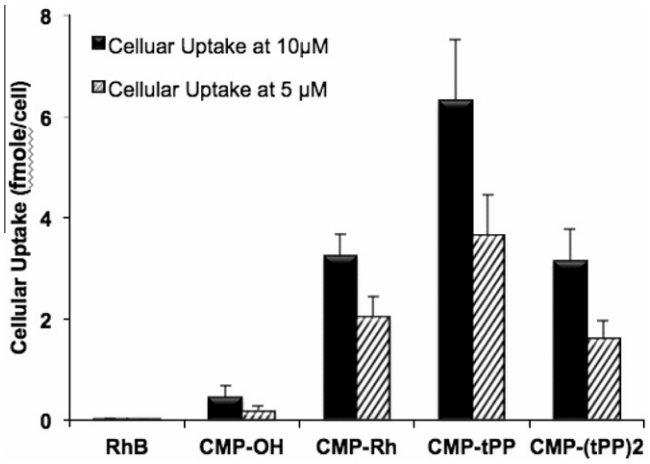

Figure 6. Intracellular accumulation of the dyes in Colon 26 cells. Cells were incubated with the respective dyes (at 5 or 10 μM) for 24 h and the intracellular uptake was determined from a fluorescence standard curve of each dye.

3. Summary and conclusion

Three conjugates, CMP-Rh, CMP-tPP, and CMP-$(tPP)_2$, were successfully synthesized by linking the hydroxy core modified porphyrins (CMP-OH and CMP-$(OH)_2$) to either rhodamine B (Rh B) or triphenyl phosphonium (tPP), respectively via a saturated hydrocarbon linker in moderate yields. Although ET from Rh to CMP

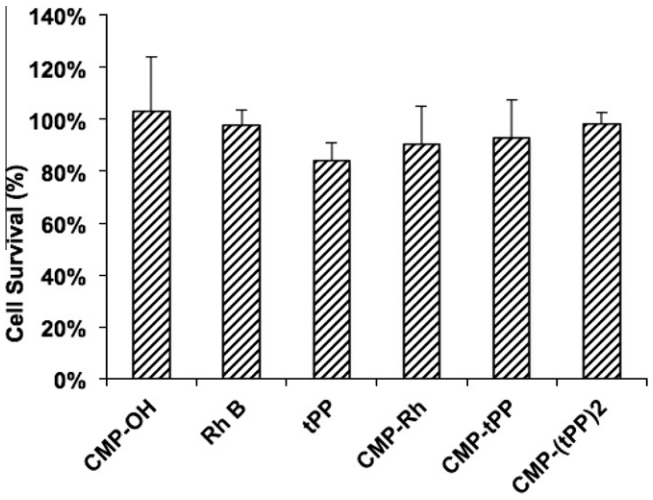

Figure 7. Dark toxicities of the respective dyes incubated in Colon 26 cells for 24 h at 5 μM concentrations.

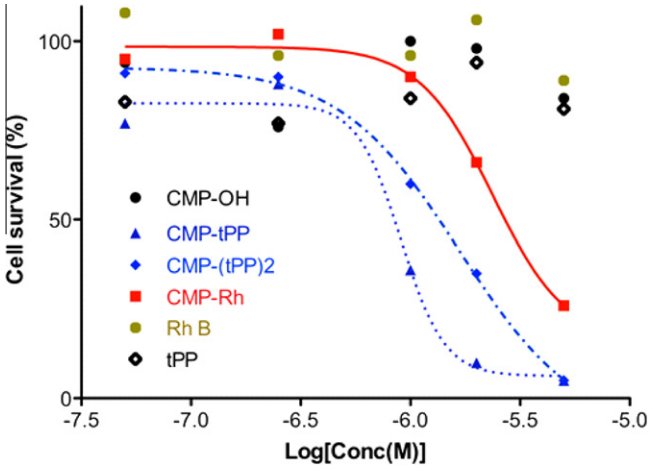

Figure 8. Phototoxicity of Colon 26 cells treated with the respective dyes and irradiated with a 690 nm diode laser for all dyes (except Rh B with 540 ± 10 nm LumaCare) at 5.6 $mWcm^{-2}$ for 30 min. Cells were incubated with the respective dyes at 0.25, 0.5, 1, 2 and 5 μM, respectively for 24 h prior to irradiation. Each data point is the average of two independent experiments with more than four data and error bars are not shown for clarity.

was observed in CMP-Rh, it was able to generate singlet oxygen at a rate comparable to that of CMP-OH. The conjugation of CMP to Rh and tPP did greatly improve intracellular uptake and in vitro photodynamic activity compared to CMP-OH. The high phototoxicity of the conjugates could be attributed to their intracellular accumulation. Our goal was to deliver CMP to mitochondria by conjugating it with DLCs (Rh or tPP). Rh moiety seemed an excellent delivery vector for CMP to mitochondria. Di-tPP group also delivered it to mitochondria somewhat but mono tPP group was not effective. However, it was not clear if the mitochondrial localization can enhance phototoxicity with our results. Although CMP-Rh showed the most preferential localization into mitochondria among the three, it was less potent than the other two conjugates.

4. Experimental section

4.1. General methods

All solvents and reagents were used as obtained from Sigma–Aldrich and Thermo Fisher Scientific unless otherwise stated. All reactions were monitored by TLC using 5–17 μm silica gel plates with fluorescent indicators from Sigma–Aldrich. All column chromatography was done using 40–63 μm silica gel from Sorbent Technologies. NMR spectra were recorded at 25 °C using a Brukner AVANCE 400 spectrometer or a Varian Mercury 300 spectrophotometer. Residual solvent signals were used as internal standards in ^1H NMR. Elemental analyses were performed by Atlantic Microlabs Inc. ESI mass spectrometry was performed either at the University of Oklahoma Mass Spectrometry Facility or at of the University of Buffalo's Chemistry Department's Instrument Center.

4.2. Synthesis

4.2.1. Synthesis of compounds 1 and 2

Compounds **1** and **2** were synthesized and characterized according to the method used in the reference.[42]

4.2.2. Synthesis of 5,10,15-triphenyl-20-(3-bromopropyl phenyl ether)-21,23-dithiaporpyrin (3)

To a solution porphyrin (**1**) (500 mg, 0.74 mmol) and 1,3-dibromopropane (1.6 mL) in acetone (40 mL) was added K_2CO_3 (1222 mg, 8.83 mmol) and refluxed at 80 °C for 36 h. K_2CO_3 was filtered off from the cooled reaction mixture. Then, the filtrate was concentrated under reduced pressure and purified over silica gel column chromatography using hexane/ethyl acetate (70:30) as an eluent to afford **3** as purple crystals (450 mg, 76% yield).[23] ^1H NMR (300 MHz, $CDCl_3$) δ 2.52 (m, 2H) 3.79 (m, 2H), 4.40 (m, 2H), 7.36 (m, 2H, 8.4 Hz) 7.84 (br s, 9H), 8,18 (m, 2H, 8.4 Hz), 8.26 (d, 6H, J = 5.6 Hz), 8.69 (s, 3H), 8.72 (d, 1H, J = 4.4 Hz), 9.69 (s, 3H), 9.73 (d, 1H, J = 4.8 Hz); HRMS (TOF MS ES+) Calculated for $[C_{47}H_{34}BrN_2OS_2]^+$, $(M^*)^+$ 785.1296. Found 785.1284.

4.2.3. Synthesis of compound 4 (CMP-tPP)

The compound was synthesized according to the method used for the synthesis of triphosphonium cations.[50] To synthesizes CMP-tPP cation bromide (**4**), triphenyl phosphine [38 mg, 0.15 mmol], alkylated CMP (**3**) (103 mg, 0.13 mmol) and absolute ethanol (25 mL) were charged into a one necked round bottomed flask equipped with a condenser, sealed with aluminum foil and stirred under reflux at 85 °C for 88 h. Removal of the solvent under reduced pressure gave a purple-black precipitate, which was then dissolved in CH_2Cl_2 (2 mL). Addition of diethyl ether (30 ml) gave a suspension. After 5 min, the supernatant was filtered. The CH_2Cl_2/diethyl ether extraction procedure was repeated three more times to remove the excess triphenyl phosphine and the residual solvent removed under reduced pressure to afford **4** as brownish solid (60 mg, 47 % yield). ^1H NMR (300 MHz, $CDCl_3$) δ 2.34 (br s, 2H), 4.0 8(br s 2H), 4.54 (br s 2H), 7.35 (br d, 2H) 7.62-8.02 (br m, 24H), 8.15 (br d, 2H), 8.25 (m, 6H), 8.70 (br s, 4H), 9.72 (br s, 4H). HRMS (ESI) Calculated for $[C_{65}H_{48}N_2OP_2]^+$, $(M^*)^+$ 967.2927. Found 967.2923; Elemental analysis Calculated for $C_{65}H_{48}BrN_2OPS_2$. $3.5H_2O$: C, 70.26; H, 4.99; N, 2.52. Found: C, 70.28; H, 4.83; N, 2.58.

4.2.4. Synthesis of compound 5

A mixture of porphyrin **2** (400 mg, 0.59 mmol), K_2CO_3 (1170 mg, 8.46 mmol) and 1, 3-dibromopropane (1.6 mL) in 20 mL of acetone was treated as described for compound **3** to afford **5** (420 mg, 77.7% yield) as a purple solid. ^1H NMR (300 MHz, $CDCl_3$) δ 2.52 (m, 4H), 3.78 (m, 4H), 4.40 (m, 4H), 7.34 (d, 4H, J = 8.1 Hz), 7.79 (m, 6H), 8.17 (AA′, 4H, J = 8.1 Hz), 8.24 (m, 4H), 8.67 (d, 2H, J = 4.5 Hz), 8.71 (d, 2H, J = 4.4 Hz), 9.76 (s, 2H), 9.72 (s, 2H). HRMS (TOF MS ES+) Calculated for $[C_{50}H_{39}Br_2N_2O_2S_2]^+$, $(M^*)^+$ 921.0820. Found 921.0853.

4.2.5. Synthesis of compound 6 [CMP-$(tPP)_2$]

The same procedure used for the synthesis of **4** was used for the synthesis of CMP-$(tPP)_2$ dication **(6)**. tPP (1639 mg, 10 mmol),

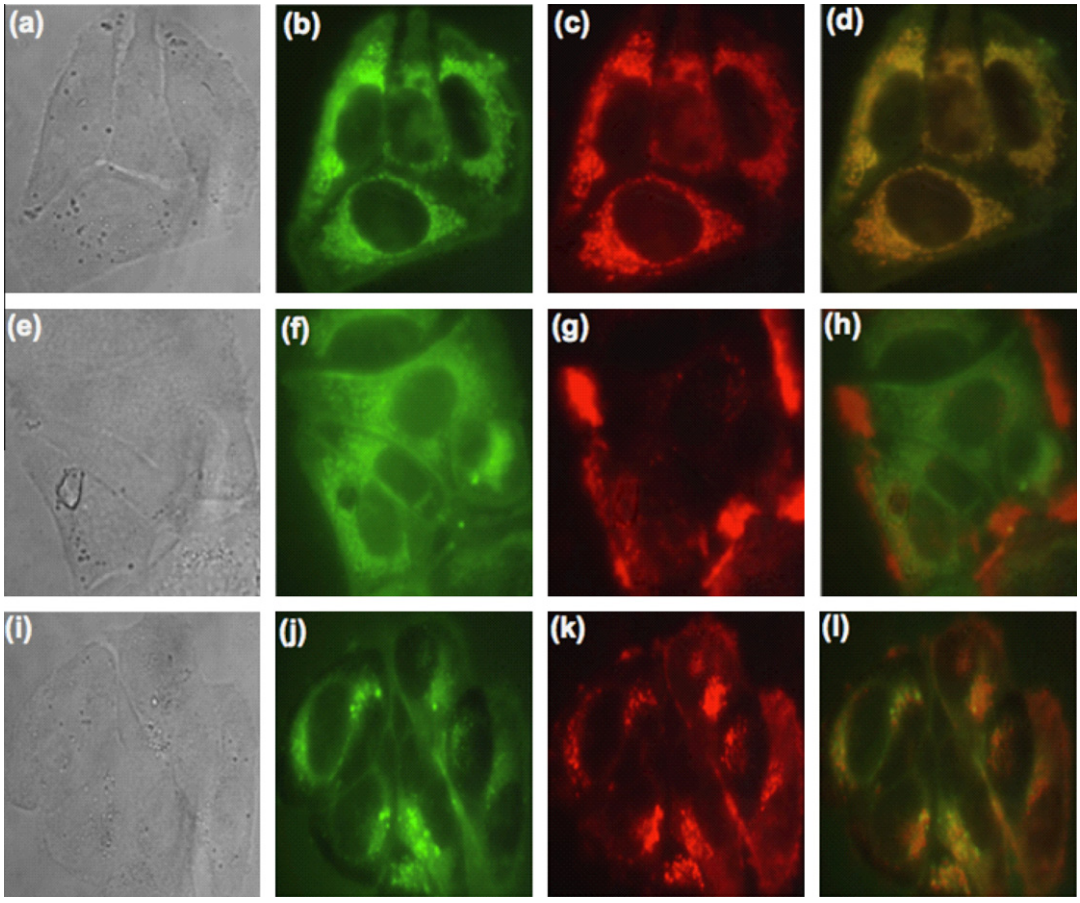

Figure 9. Sub-cellular localization of the conjugates: MCF-7 cells treated with Rh 123 and one of the conjugates. ***CMP-Rh + Rh 123*** (5 μM + 2 μM) (a) Bright field (b) Green filter (c) Red filter, and (d) overlap of (b) and (c); ***CMP-tPP + Rh 123*** (5 μM + 2 μM) (e) Bright field (f) Green filter (g) Red filter, and (h) overlap of (f) and (g); ***CMP-(tPP)2 + Rh 123*** (5 μM + 2 μM) (i) Bright field (j) Green filter (k) Red filter, and (l) overlap of (j) and (k).

dialkylated-CMP, **5** (577 mg, 0.63 mmol) in 10 mL of absolute ethanol were stirred under reflux for 96 h at 85 °C. After complete removal of excess tPP following the dissolution in minimal CH_2Cl_2, precipitation using diethyl ether and filtration using sinter funnel, the solid residue constituting of the mixture mono and dications were then separated using silica gel column chromatography using CH_2Cl_2:MeOH (80:20) as eluent to afford **6** as a brownish solid (200 mg, 22% yield). It seemed that most of the compound was lost during the column chromatography. HRMS (ESI) Calculated for $[C_{86}H_{68}N_2O_2P_2S_2]^{2+}$, $(M^*)^{2+}$ 643.2093, and for $(M^*)^{3+}$ 429.1420. Found 643.2088 and 429.1426 respectively; Elemental analysis Calculated for $C_{86}H_{68}Br_{1.85}N_2O_2P_2S_2$. $5.2H_2O$: C, 67.55; H, 5.17; Br, 9.67; N, 1.83. Found: C, 67.22; H, 4.91; Br, 9.24; N, 1.67.

4.2.6. Synthesis of compound 7

To a solution of **3** (150 mg, 0.19 mmol) in anhydrous DMF (4 mL) was added anhydrous sodium acetate (78 mg, 0.95 mmol).[51] The solution was heated to 90 °C for 12 h. Water (50 mL) and ethyl acetate (100 mL) were then added. The organic layer was separated, washed with saturated ammonium chloride, then with water and finally with brine and then dried over anhydrous Na_2SO_4. The solvent was evaporated under reduced pressure and column chromatography was performed using 100 % CH_2Cl_2 to afford **7** (110 mg, 78%) as purple crystals crashed of the solution using dry hexane. ^{1}H NMR (300 MHz, $CDCl_3$) δ 2.16 (s, 3H), 2.32 (m, 2H), 4.34 (t, 2H, J = 6.21 Hz), 4.45 (t, J = 6.18 Hz), 7.36 (d, 2H, J = 8.4 Hz), 7.84 (s, 9H), 8,18 (d, 2H, J = 8.4 Hz), 8.26 (d, 6H, J = 5.6 Hz), 8.44 (br d, 1H), 8.70 (br s, 4H), 9.71 (br s, 4H). HRMS (ESI) Calculated for $[C_{49}H_{36}N_2O_3S_2+H]^+$ 765.2246. Found 765.2264.

4.2.7. Synthesis of compound 8

To a stirring solution of compound **7** (110 mg, 0.14 mmol) in 4.5 mL mixture of THF:MeOH:H_2O (v/v/v; 1.3:2.5:0.75) was added 2 mL of 0.5 N NaOH aqueous solution into a two necked round bottom flask and refluxed at 80 °C overnight. The reaction was quenched with water (20 mL). Organic solvents were removed under reduced pressure, and the residue was extracted with ethyl acetate (3 × 50 mL). The combined layers were washed with 2 N HCl (2 × 20 mL), followed by washings with water and then with brine and dried over Na_2SO_4. The extract was concentrated to dryness to afford a dark brown solid (90 mg, 87 % yield) and used without further purification for the next step. ^{1}H NMR (300 MHz, $CDCl_3$) δ 2.22 (m, 2H), 4.01 (t, 2H, J = 6 Hz), 4.39 (t, 2H, J = 6.21 Hz), 7.36 (d, 2H, J = 8.4 Hz) 7.84 (s, 9H), 8,18 (d, 2H, J = 8.4 Hz), 8.26 (d, 6H, J = 5.6 Hz), 8.44 (br d, 1H), 8.70 (br s, 4H), 9.71 (br s, 4H). HRMS (ESI) Calculated for $[C_{47}H_{34}N_2O_2S_2+H]^+$ 723.2140. Found 723.2160.

4.2.8. Synthesis of compound 9 (CMP-Rh)

To a stirred solution of Rhodamine B (72 mg, 0.15 mmol) in anhydrous CH_2Cl_2 (2 mL) was added DMAP (1.85 mg, 0.015 mmol) and **8** (100 mg, 0.14 mmol). DCC (32 mg, 0.15 mmol) in CH_2Cl_2 (1 mL) was added to the reaction mixture at 0 °C, which was then stirred for 10 min at 0 °C and 72 h at room temperature. Precipitated urea was then filtered off using cooled CH_2Cl_2 and the filtrate evaporated in vacuo. The residue was taken up in CH_2Cl_2 and filtered free of any precipitated urea. The CH_2Cl_2 solution was washed twice with 0.5 N HCl followed with saturated $NaHCO_3$ solution, and then dried over anhydrous Na_2SO_4. The solvent was

removed by evaporation and the ester isolated by silica gel column chromatography using CH_2Cl_2:MeOH (95:5) as the eluent to afford **9** as a dark blue solid (60 mg, 38% yield). ^{1}H NMR (300 MHz, $CDCl_3$) δ 1,26 (t, 12H, J = 7.02 Hz), 2.15 (m, 2H), 3.55 (q, 8H, J = 7.03 Hz), 4.17 (t, 2H, J = 6 Hz), 4.38 (t, J = 6.21 Hz), 6.76–6.91 (m, 4H), 7.15 (d, 2H, J = 8.7 Hz), 7.26 (d, 2H, J = 9.9 Hz), 7.36 (br d, 1H) 7.84 (br s, 11H), 8,18 (d, 2H, J = 8.4 Hz), 8.26 (d, 6H, J = 5.6 Hz), 8.44 (br d, 1H), 8.70 (br s, 4H), 9.71 (br s, 4H). HRMS (ESI) Calculated for $[C_{75}H_{63}N_4O_4S_2]^+$ $(M^*)^+$ 1147.4291. Found 1147.4271; Elemental analysis Calculated for $C_{75}H_{63}Cl_{0.7}N_4O_4S_2$. $7H_2O$: C, 69.33; H, 5.97; Cl, 1.91; N, 4.31; Found: C, 69.70; H, 6.69; Cl, 2.23; N, 3.25.

4.3. Photophysical studies

The photophysical properties of the synthesized conjugates and their corresponding components were determined in either chloroform or dimethyl sulphoxide. Electronic absorption spectra were recorded using either a PerkinElmer UV–Vis spectrophotometer (LAMBDA 25). Steady state fluorescence spectra were recorded with a PerkinElmer fluorescence spectrometer LS45 or a Molecular Device fluorescence plate reader (Gemini EM).

4.3.1. Absorption spectra and molar extinction coefficients

The molar extinction coefficients were calculated from serially diluted solutions and results were reported in $M^{-1}\,cm^{-1}$.

4.3.2. *n*-Octanol/pH 7.4 buffer partition coefficients

n-Octanol/water partition coefficients of the dyes were determined by the 'shake flask' direct measurement method.[52] Saturated solutions of the dyes were prepared by adding the dyes to a mixture of equal volumes (1 mL) of *n*-octanol and a pH 7.4 phosphate buffer. The saturated solutions were placed in an ultrasound bath for 30 min, then left to settle for 4 h. Then, each layer was diluted with chloroform and the absorbance of the dyes in the respective solutions was determined. The partition coefficients were then obtained by calculating the ratio of the concentrations of the respective dyes in the two layers ([Dye]*n*-octanol/[Dye]buffer). Results were reported as $\log D_{7.4}$ values.

4.3.3. Aggregation tendency of the dyes in a medium

Tendency of the dyes to aggregate in a culture medium was indirectly determined by comparing their fluorescence intensities in the culture medium to that in DMSO.[40] The dyes were dissolved in DMSO (2 mM), diluted to the appropriate concentrations with more DMSO, and 10 μL of the diluted solution added to 190 μL of either complete media or DMSO in 96 well plates to give 10 μM solutions. The plates were then left for an hour after which the fluorescence readings were taken at the appropriate excitation and emission wavelengths (CMPOH, CMP-tPP, CMP-$(tPP)_2$ excitation 410 nm, emission 714 nm, CMP-Rh, Rh B excitation 520 nm, emission 590). The change in the fluorescence intensities of the dyes in a complete medium compared to that in DMSO was then used to estimate the aggregation tendencies of the dyes. The results were expressed in arbitrary units.

4.3.4. ET in the CMP-Rh conjugate

Due to the proximity of the two fluorophores, CMP-Rh was expected to act as a ET pair where Rh B acts as the donor and CMP acts as acceptor. Thus, it was necessary to determine the ET efficiency to estimate the SO generating capability of the conjugate. Decrease in fluorescence intensities of the donor molecule at specific wavelengths, measured in the presence of the acceptor molecule at different distances, was used to demonstrate ET in the conjugate.[53] A solution of the conjugate (molecules in a close proximity) and an equimolar mixture of the conjugate's individual components CMP-OH and Rh B (molecules at a long range) were compared. Stock solutions of the CMP-Rh, CMP and Rh B (2 mM) were prepared in THF. The compound stock solutions were then diluted with THF to give 1 μM solutions. The fluorescence intensities of CMP-Rh and a mixture of CMP-OH and Rh B were measured by exciting at 435 and 525 nm and the fluorescence was measured from 535–650 nm to or 500–750 nm. The decrease in fluorescence intensity of the Rh B peak at 580 nm was used to demonstrate ET.

4.3.5. Singlet oxygen generation

The generation of singlet oxygen by the respective dyes upon irradiation was determined indirectly, by measuring the rates of oxidation of 1,3-diphenylisobenzofuran (DPBF).[54,55] Stock solutions of the respective dyes (2 mM) were prepared in DMSO. A solution of the respective photosensitizer (5 μM) and DPBF (100 μM) in THF were then prepared in culture tubes, so that the 2 mL solutions had not more than 2% (v/v) of DMSO as a cosolvent. The culture tubes were then irradiated using 690 ± 10 nm light (LC122-A, LumaCare) for all the dyes at 1 $mWcm^{-2}$ for 20 min. Every 2 min, the absorption readings at 414 nm were taken. The rates of DPBF oxidation by the different dyes were then compared.

4.4. Biological studies

4.4.1. Cells and culture conditions

Mouse colon cancer cells (Colon 26) or human breast cancer cells (MCF-7) were used for all biological experiments. All reagents and culture media were obtained from Invitrogen and Sigma–Aldrich. The cells were maintained in minimum essential medium (α-MEM) supplemented with 10% bovine growth serum, 2 mM L-glutamine, 50 units/mL penicillin G, 50 μg/mL streptomycin and 1.0 μg/mL fungizone. The cells were incubated at 37 °C in 5 % CO_2 using a Sanyo MCO-18AIC-UV incubator. Colon 26 cells were sub-cultured biweekly and MCF-7 cells were sub-cultured once a week to maintain the cells at approximately 80% confluency. The dyes in all studies were initially dissolved in DMSO to make a 2 mM stock solution. A Lab-line Barnstead International orbital shaker was used for all phototoxicity tests to make more homogeneous light exposure. A BioTek® plate reader (Synergy™ 2) was used to read UV/Vis absorbance. A Molecular Device fluorescence plate reader (Gemini EM) was used to read the fluorescence.

4.4.2. Intracellular accumulation

Dye concentrations in cells were determined using the fluorescence intensities of the dyes at appropriate excitation and emission wavelengths, following the procedures in our previous reports.[29,56] Intracellular accumulation at treatment concentrations 10 and 5 μM were determined.

4.4.3. Dark toxicity

The cells were treated and cell viability was determined as described in the experimental section for phototoxicity without irradiation at 5 μM concentration.[29]

4.4.4. Phototoxicity

Colon 26 cells were seeded at 1–1.5 × 10^4 cells/well in 96 well plates then incubated for 24 h in 5% CO_2 at 37 °C. The stock solutions of the dyes (2 mM in DMSO) were diluted to appropriate concentrations with the complete medium and added to the cells to give final dye concentrations (0.25, 0.5, 1, 2, 5 μM). After incubation for 24 h, the medium was removed and the cell monolayer was rinsed twice with 190 μL of a 0.9% NaCl solution. The complete medium was then added to the wells and the well plate was placed on the well plate shaker. The well plate lids were removed and the wells were exposed to 690 nm diode laser (except Rh B with 540 ± 10 nm LumaCare) delivered at 5.6 $mWcm^{-2}$ for 30 min. To achieve more uniform irradiation, the entire well plate was gently

orbited on the shaker. After the irradiation, the cells were again incubated for 24 h, after which the cytotoxicity was determined by MTT assay and expressed as a percent of the controls (cells exposed to light in the absence of the dyes).

4.4.5. Sub-cellular localization

General procedures for image slide preparation: Cells were seeded at $2–3 \times 10^4$ cells/well in 24 well plates containing one 12 mm diameter cover slip per well and then incubated for 24 h. The dyes diluted to the appropriate concentrations were then added to the well plates and incubated for 14 h. [For dual imaging with Rh-123, 2 μM of Rh-123 was added to the cells at 12 h time point and the cells incubated for 2 more hours.] After 14 h the media was removed and the cell monolayer rinsed three times with 1 mL of PBS solution. The cover slip was then mounted on a slide and the images were taken using a Leica DMI4000B fluorescence microscope fitted with a QImaging Fast 1394 camera and spot advance version 4.6 processing software. The images were processed for better visualization with Adobe Photoshop Element 5.0.

Dual staining of each dye with Rh-123 (Rhodamine 123, M-7514 from Sigma–Aldrich) was made to determine their mitochondrial localization. Since both CMP-OH and the conjugates (CMP-tPP, CMP-$(tPP)_2$ and CMP-Rh) fluoresce in the red region of the optical spectrum, a red filter (Propidium Iodide filter, exciter: HQ535/50; emitter: HQ645/75; set: 41005 from Chroma Technology Co.) was used to acquire the images. For Rh123, which fluoresces in the green region of the optical spectrum, the images were obtained using a green filter (FTC/Bdipy/Fluo3/DiO filter, exciter: HQ480/40; emitter: HQ535/50; set: 41001 from Chroma Technology Co.). To determine the appropriate exposure times, the minimum time required to take an image of cells individually stained with Rh-123, CMP-Rh, CMP-tPP, or CMP-$(tPP)_2$ were obtained from the independent experiments. For dual staining experiments, the cells were stained with Rh-123 and either CMP-Rh, CMP-tPP or CMP-$(tPP)_2$ and images were obtained using both the green and red filters. The green and red images were then superimposed, and the regions of colocalization appeared as yellow.

4.5. Statistical analyses

Statistical analyses were performed using the Student's *t*-test for pairwise comparisons. A P value of <0.05 was considered significant. The Hill (sigmoid E_{max}) equation was used to determine IC_{50} values.

Acknowledgments

This research was supported by the College of Pharmacy, University of Oklahoma. We would also like to thank Mr. Arto Baghdayan at OUHSC for his technical guidance with the fluorescence microscope.

References and notes

1. Detty, M. R. *Expert Opin. Ther. Pat.* **1849**, *2001*, 11.
2. Sharman, W. M.; Allen, C. M.; van Lier, J. E. *Drug Discovery Today* **1999**, *4*, 507.
3. Moan, J.; Berg, K. *Photochem. Photobiol.* **1991**, *53*, 549.
4. Kroemer, G.; Reed, J. C. *Nat. Med.* **2000**, *6*, 513.
5. Reed, J. C. *Am. J. Pathol.* **2000**, *157*, 1415.
6. Kroemer, G.; Dallaporta, B.; Resche-Rigon, M. *Annu. Rev. Physiol.* **1998**, *60*, 619.
7. Costantini, P.; Jacotot, E.; Decaudin, D.; Kroemer, G. *J. Natl. Cancer Inst.* **2000**, *1042*, 92.
8. Gottlieb, R. A. *FEBS Lett.* **2000**, *482*, 6.
9. Green, D. R. *Cell* **2000**, *102*, 1.
10. Qin, Z. H.; Wang, Y.; Kikly, K. K.; Sapp, E.; Kegel, K. B.; Aronin, N.; DiFiglia, M. *J. Biol. Chem.* **2001**, *276*, 8079.
11. Morgan, J.; Oseroff, A. R. *Adv. Drug Deliv. Rev.* **2001**, *49*, 71.
12. Peng, T. I.; Chang, C. J.; Guo, M. J.; Wang, Y. H.; Yu, J. S.; Wu, H. Y.; Jou, M. J. *Ann. N. Y. Acad. Sci.* **2005**, *1042*, 419.
13. Modica-Napolitano, J. S.; Aprille, J. R. *Cancer Res.* **1987**, *47*, 4361.
14. Sun, X.; Wong, J. R.; Song, K.; Hu, J.; Garlid, K. D.; Chen, L. B. *Cancer Res.* **1994**, *54*, 1465.
15. Modica-Napolitano, J. S.; Koya, K.; Weisberg, E.; Brunelli, B. T.; Li, Y.; Chen, L. B. *Cancer Res.* **1996**, *56*, 544.
16. Rodriguez, M. E.; Azizuddin, K.; Zhang, P.; Chiu, S. M.; Lam, M.; Kenney, M. E.; Burda, C.; Oleinick, N. L. *Mitochondrion* **2008**, *8*, 237.
17. Sibrian-Vazquez, M.; Nesterova, I. V.; Jensen, T. J.; Vicente, M. G. *Bioconjug. Chem.* **2008**, *19*, 705.
18. Dias, N.; Bailly, C. *Biochem. Pharmacol.* **2005**, *70*, 1.
19. Dummin, H.; Cernay, T.; Zimmermann, H. W. *J. Photochem. Photobiol. B* **1997**, *37*, 219.
20. Modica-Napolitano, J. S.; Aprille, J. R. *Adv. Drug Deliv. Rev.* **2001**, *49*, 63.
21. Wang, F.; Ogasawara, M. A.; Huang, P. *Mol. Aspects Med.* **2010**, *31*, 75.
22. Davis, S.; Weiss, M. J.; Wong, J. R.; Lampidis, T. J.; Chen, L. B. *J. Biol. Chem.* **1985**, *260*, 13844.
23. Ngen, E. J.; Rajaputra, P.; You, Y. *Bioorg. Med. Chem.* **2009**, *17*, 6631.
24. Stilts, C. E.; Nelen, M. I.; Hilmey, D. G.; Davies, S. R.; Gollnick, S. O.; Oseroff, A. R.; Gibson, S. L.; Hilf, R.; Detty, M. R. *J. Med. Chem.* **2000**, *43*, 2403.
25. Hilmey, D. G.; Abe, M.; Nelen, M. I.; Stilts, C. E.; Baker, G. A.; Baker, S. N.; Bright, F. V.; Davies, S. R.; Gollnick, S. O.; Oseroff, A. R.; Gibson, S. L.; Hilf, R.; Detty, M. R. *J. Med. Chem.* **2002**, *45*, 449.
26. You, Y. J.; Gibson, S. L.; Hilf, R.; Davies, S. R.; Oseroff, A. R.; Roy, I.; Ohulchanskyy, T. Y.; Bergey, E. J.; Detty, M. R. *J. Med. Chem.* **2003**, *46*, 3734.
27. You, Y. J.; Gibson, S. L.; Hilf, R.; Ohulchanskyy, T. Y.; Detty, M. R. *Bioorg. Med. Chem.* **2005**, *13*, 2235.
28. You, Y. J.; Gibson, S. L.; Detty, M. R. *Bioorg. Med. Chem.* **2005**, *13*, 5968.
29. Ngen, E. J.; Daniels, T. S.; Murthy, R. S.; Detty, M. R.; You, Y. *Bioorg. Med. Chem.* **2008**, *16*, 3171.
30. Bellnier, D. A.; Dougherty, T. J. *J. Clin. Laser Med. Surg.* **1996**, *14*, 311.
31. Zhao, Z.; Chan, P. S.; Li, H.; Wong, K. L.; Wong, R. N.; Mak, N. K.; Zhang, J.; Tam, H. L.; Wong, W. Y.; Kwong, D. W.; Wong, W. K. *Inorg. Chem.* **2012**, *51*, 812.
32. Murphy, M. P. *Trends Biotechnol.* **1997**, *15*, 326.
33. Muratovska, A.; Lightowlers, R. N.; Taylor, R. W.; Wilce, J. A.; Murphy, M. P. *Adv. Drug Deliv. Rev.* **2001**, *49*, 189.
34. Filipovska, A.; Eccles, M. R.; Smith, R. A.; Murphy, M. P. *FEBS Lett.* **2004**, *556*, 180.
35. James, A. M.; Sharpley, M. S.; Manas, A. R.; Frerman, F. E.; Hirst, J.; Smith, R. A.; Murphy, M. P. *J. Biol. Chem.* **2007**, *282*, 14708.
36. Xu, W.; Chen, H.; Wang, Y.; Zhao, C.; Li, X.; Wang, S.; Weng, Y. *ChemPhysChem* **2008**, *9*, 1409.
37. Wu, J. J.; Li, N.; Li, K. A.; Liu, F. *J. Phys. Chem. B* **2008**, *112*, 8134.
38. Chen, Y.; Gryshuk, A.; Achilefu, S.; Ohulchansky, T.; Potter, W.; Zhong, T.; Morgan, J.; Chance, B.; Prasad, P. N.; Henderson, B. W.; Oseroff, A.; Pandey, R. K. *Bioconjug. Chem.* **2005**, *16*, 1264.
39. Mohanty, J.; Nau, W. M. *Angew. Chem., Int. Ed.* **2005**, *44*, 3750.
40. Moser, J. G. *Photodynamic Tumor Therapy: 2nd and 3rd Generation Photosensitizers*; Harwood Academic Publishers: Amdterdam, 1998.
41. Krieg, M. *J. Biochem. Biophys. Methods* **1993**, *27*, 143.
42. You, Y.; Gibson, S. L.; Hilf, R.; Davies, S. R.; Oseroff, A. R.; Roy, I.; Ohulchanskyy, T. Y.; Bergey, E. J.; Detty, M. R. *J. Med. Chem.* **2003**, *46*, 3734.
43. You, Y.; Gibson, S. L.; Hilf, R.; Ohulchanskyy, T. Y.; Detty, M. R. *Bioorg. Med. Chem.* **2005**, *13*, 2235.
44. You, Y.; Gibson, S. L.; Detty, M. R. *Bioorg. Med. Chem.* **2005**, *13*, 5968.
45. Modica-Napolitano, J. S.; Aprille, J. R. *Adv. Drug Deliv. Rev.* **2001**, *49*, 63.
46. Mislick, K. A.; Baldeschwieler, J. D. *Proc. Natl. Acad. Sci. U.S.A.* **1996**, *93*, 12349.
47. Dias, N.; Bailly, C. *Biochem. Pharmacol.* **2005**, *70*, 1.
48. Morgan, J.; Oseroff, A. R. *Adv. Drug Deliv. Rev.* **2001**, *49*, 71.
49. Navia, M. A.; Chaturvedi, P. R. *Drug Discovery Today* **1996**, *1*, 179.
50. James, A. M.; Blaikie, F. H.; Smith, R. A.; Lightowlers, R. N.; Smith, P. M.; Murphy, M. P. *Eur. J. Biochem.* **2003**, *270*, 2827.
51. Kaufhold, M. EP0294557, **1988**.
52. Leo, A.; Hansch, C.; Elkins, D. *Chem. Rev.* **1971**, *71*, 525.
53. Lakowitcz, J. R. *Principles of Fluorescence Spectrocopy*; Springer Publishing Company: Chicago, 2006. Chapter 9.
54. Spiller, W.; Kliesch, H.; Wöhrle, D.; Hackbarth, S.; Röder, B.; Schnurpfeil, G. *J. Porphyrins Phthalocyanines* **1998**, *2*, 145.
55. Yogo, T.; Urano, Y.; Ishitsuka, Y.; Maniwa, F.; Nagano, T. *J. Am. Chem. Soc.* **2005**, *127*, 12162.
56. You, Y.; Gibson, S. L.; Detty, M. R. *J. Photochem. Photobiol. B* **2006**, *85*, 155.